Journal of The Electrochemical Society, 152 (6) G500-G505 (2005)
0013-4651/2005/152(6)/G500/6/$7.00 © The Electrochemical Society, Inc.

# Boron Segregation in Single-Crystal $Si_{1-x-y}Ge_xC_y$ and $Si_{1-y}C_y$ Alloys

**E. J. Stewart,[a,b,z] M. S. Carroll,[a,c] and J. C. Sturm***

[a]*Center for Photonics and Optoelectronic Materials, Department of Electrical Engineering, Princeton University, Princeton, New Jersey 08544, USA*

It has been reported that boron segregates to single-crystal $Si_{1-x}Ge_x$ layers from silicon during thermal anneals. In this work, we find that boron segregates even more strongly into single-crystal $Si_{1-x-y}Ge_xC_y$, as has been previously reported for polycrystalline films. This effect is also observed in single-crystal $Si_{1-y}C_y$. Segregation coefficients range from 1.7 to 2.9 for annealing temperatures in the 800-850°C range. In a $Si_{1-y}C_y$ layer with 0.4% carbon, most of the segregation is reversible if the carbon is removed by an oxidation-enhanced out-diffusion process. This argues against the formation of immobile B-C defects as the driving force for the segregation. Gradients of interstitial silicon atoms, created by high concentrations of substitutional carbon, are presented as a driving force capable of causing the segregation seen in the experiments.
© 2005 The Electrochemical Society. [DOI: 10.1149/1.1915209] All rights reserved.

Manuscript submitted January 16, 2004; revised manuscript received January 5, 2005. Available electronically May 11, 2005.

$Si_{1-x-y}Ge_xC_y$ and $Si_{1-y}C_y$ alloys are of great interest for controlling dopant diffusion in silicon-based devices. It has been shown that by adding small amounts of substitutional carbon (~0.1-1.0%) to silicon or $Si_{1-x}Ge_x$, the diffusivity of boron and phosphorus atoms can be reduced by an order of magnitude below normal levels.[1] This is useful for devices where very sharp dopant profiles must be created and then maintained during subsequent high-temperature fabrication steps. $Si_{1-x-y}Ge_xC_y$ has been used most notably as a base material for a heterojunction bipolar transistor;[2] other potential applications include metal oxide semiconductor field effect transistor (MOSFET) channels and source/drains.[3,4]

In addition to reducing diffusion, carbon has also been shown to induce boron segregation. In polycrystalline $Si/Si_{1-x-y}Ge_xC_y$ multilayer structures with carbon levels ranging from 0.05-1.5%, boron strongly segregates from the polysilicon layers into the polycrystalline $Si_{1-x-y}Ge_xC_y$ during 800-900°C thermal anneals.[5] Segregation increases with increasing carbon level, and can be much stronger than previously reported segregation to single-crystal $Si_{1-x}Ge_x$.[6,7] This effect provides additional control over dopant profiles, as boron not only diffuses more slowly but is also drawn into carbon-containing regions. It has been exploited in the gates of p-channel MOSFETs, where devices with polycrystalline $Si_{1-x-y}Ge_xC_y$ layers in the gates show increased resistance to boron penetration effects (and thus enhanced threshold voltage stability) due to the suppression of boron out-diffusion from the gate.[8]

In this work, we study boron segregation in single-crystal $Si_{1-x-y}Ge_xC_y$ and $Si_{1-y}C_y$. We find that, similar to the polycrystalline case, boron accumulates in both $Si_{1-x-y}Ge_xC_y$ and $Si_{1-y}C_y$ layers (*vs.* Si) during thermal anneals. The segregation process is shown to be mostly reversible by removing the carbon from the $Si_{1-y}C_y$ layer. Driving mechanisms for the segregation are discussed in light of this data. Interstitial gradients, created by out-diffusion of substitutional carbon, are then presented as a driving mechanism for segregation.

## Boron Segregation to Single-Crystal $Si_{1-x-y}Ge_xC_y$ and $Si_{1-y}C_y$

All samples used in this study were grown by rapid thermal chemical vapor deposition using $SiCl_2H_2$ and $Si_2H_6$ as silicon sources and $GeH_4$, $SiCH_6$, and $B_2H_6$ as sources for germanium, carbon, and boron, respectively. $Si_{1-x-y}Ge_xC_y$ and $Si_{1-y}C_y$ layers were grown at 625°C, and silicon was deposited at temperatures ranging from 625 to 750°C. Previous work shows that for films grown under similar conditions most of the carbon is incorporated substitutionally.[9,10] Two structures were used to study segregation in single-crystal $Si_{1-x-y}Ge_xC_y$, shown in Fig. 1. For the first sample (Fig. 1a), thin (15 nm) epitaxial layers of $Si_{0.8}Ge_{0.2}$ and $Si_{0.79}Ge_{0.2}C_{0.01}$ were sandwiched between thicker (100 nm) *in situ* doped Si layers ($[B] = 2 \times 10^{19}\ cm^{-3}$), all on top of an n-type substrate and undoped buffer (500 nm). This structure was annealed at 800°C for 28 h to allow boron to move from the silicon into the $Si_{1-x}Ge_x$ and $Si_{1-x-y}Ge_xC_y$ layers. The second sample (Fig. 1b) was similar to the first, except that the $Si_{1-x}Ge_x$ and $Si_{1-x-y}Ge_xC_y$ layers were thicker (25 nm), initially *in situ* doped higher (not lower) than the silicon, and the carbon level was much lower (0.05%). (There were several other layers on either side of the region of interest, which did not affect our study and are not discussed here.) This sample was annealed for 18 h at 800°C. Secondary-ion mass spectroscopy (SIMS) analysis was used to measure germanium, carbon, boron, and oxygen profiles in all samples.

Figure 2 shows SIMS profiles of these two structures before and after annealing. For the first sample (Fig. 2a), the $Si_{1-x}Ge_x$ and $Si_{1-x-y}Ge_xC_y$ layers initially have much less dopant than the surrounding silicon. However, after the anneal, boron has moved into these layers and reached levels higher than the original silicon concentration. Defining a segregation coefficient *m* as the ratio of boron in the $Si_{1-x}Ge_x$ *vs.* Si after the anneal, we find $m = 1.7$ for the $Si_{1-x}Ge_x$ layer. Boron segregation to $Si_{1-x}Ge_x$ is well known, and the magnitude of this result is consistent with previous reports.[7,11] However, additional segregation occurs in the $Si_{1-x-y}Ge_xC_y$ layer ($m = 2.3$), showing that carbon enhances the effect. This confirms that the enhanced segregation seen in polycrystalline $Si_{1-x-y}Ge_xC_y$ in a previous report is not (at least exclusively) due to polycrystalline or grain boundary effects. (Note: In the as-grown profile there is a boron peak in the top Si layer at ~120 nm. This was unintentionally incorporated during growth and should not affect the rest of the experiment.)

The second sample (Fig. 2b) demonstrates a similar effect at a much lower carbon concentration (0.05%). As mentioned, the as-grown profiles show that during growth a higher boron concentration was initially placed in the $Si_{1-x}Ge_x$ and $Si_{1-x-y}Ge_xC_y$ layers than in the silicon. This would normally be expected to flatten out during the anneal. However, as shown in Fig. 2b, boron concentration in the $Si_{1-x-y}Ge_xC_y$ layer actually *increases* during the anneal, again indicating segregation. Interestingly, although the carbon concentration is much lower in this sample, the amount of segregation is higher ($m = 2.9$) than before. This is discussed later in the paper.

A third sample was grown to study boron segregation in $Si_{1-y}C_y$, whose structure and as-grown SIMS profile are shown in Fig. 3. On top of an n-type (100) substrate, an undoped 500 nm buffer layer was first grown, followed by a sandwich structure consisting of a thin (20 nm) $Si_{0.996}C_{0.004}$ layer in between two boron-doped ([B]

* Electrochemical Society Active Member.
[b] Present address: Northrop Grumman Corporation, Baltimore, Maryland 21203, USA.
[c] Present address: Sandia National Laboratories, Albuquerque, New Mexico 87185, USA.
[z] E-mail: estewart@alumni.princeton.edu

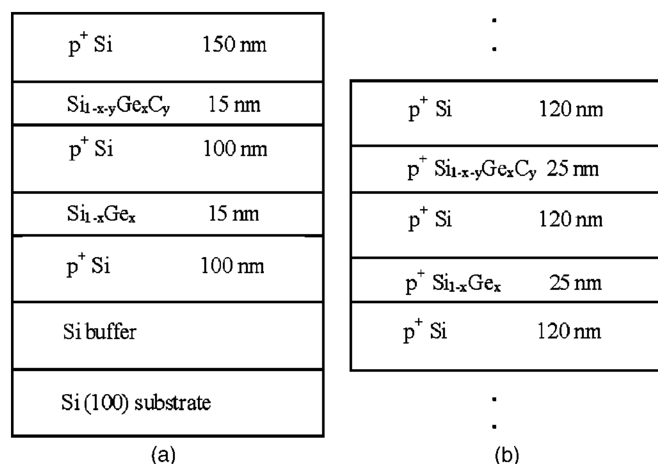


**Figure 1.** Schematic of structures used to study boron segregation in single-crystal $Si_{1-x-y}Ge_xC_y$ for (a) high-carbon content (1%) and (b) low carbon content (0.05%).

$= 2 \times 10^{19}$ $cm^{-3}$) silicon layers. The top and bottom $p^+$ silicon layers were 50 and 150 nm thick, respectively. This sample was annealed at 850°C for up to 2 h in $N_2$, and SIMS profiles were measured (Fig. 4). Similar to the $Si_{1-x-y}Ge_xC_y$ case, boron segregates into the $Si_{1-y}C_y$ layer, reaching a value 1.7 times higher than the surrounding silicon after 2 h of annealing. Some boron is also being lost from the surface of the sample due to evaporation. Oxygen concentrations, shown in both Fig. 3 and 4, are well below the boron and carbon concentrations, and no oxygen accumulation is observed in the $Si_{1-y}C_y$ layer during this anneal.

As mentioned in the introduction, boron segregation to strained $Si_{1-x}Ge_x$ (without carbon) from silicon has previously been reported. Several mechanisms have been proposed to explain this, including (*i*) small boron atoms relieving strain energy in the compressively strained $Si_{1-x}Ge_x$; (*ii*) the valence band offset, and therefore reduced hole energy, of $Si_{1-x}Ge_x$, making it energetically favorable for boron atoms (and accompanying holes) to move into the $Si_{1-x}Ge_x$ *vs.* Si; and (*iii*) direct Ge-B interactions.[12,13] However, when carbon is added to strained $Si_{1-x}Ge_x$ layers in small amounts, the carbon reduces the macroscopic compressive strain and increases the bandgap (reduces the valence band offset) compared to $Si_{1-x}Ge_x$.[14-16] Both of these observations predict less boron segregation to $Si_{1-x-y}Ge_xC_y$ layers compared to $Si_{1-x}Ge_x$, which is the opposite of what is observed. Segregation is also observed in $Si_{1-y}C_y$ layers, indicating that carbon by itself can drive the segregation (Ge-B interactions not required). Thus these mechanisms used to explain boron segregation to $Si_{1-x}Ge_x$ cannot be used to explain the segregation to $Si_{1-y}C_y$ or the enhanced segregation to $Si_{1-x-y}Ge_xC_y$ *vs.* $Si_{1-x}Ge_x$ seen here.

One possibility unique to $Si_{1-x-y}Ge_xC_y$ and $Si_{1-y}C_y$ is that boron is becoming trapped at a carbon-related defect. For example, silicon carbide (SiC) precipitates can form in $Si_{1-x-y}Ge_xC_y$ layers with carbon levels and annealing conditions similar to those used in this study,[17,18] and boron could become immobilized either inside or at the surfaces of these defects. A direct boron-carbon interaction may also be occurring, such as the B-C-I cluster proposed by Liu *et al.*[19] Either of these defects may be expected to render the boron (and carbon) atoms immobile. This possibility is considered in the next section.

## Reversibility of Boron Segregation

If boron is becoming immobilized at carbon-related defects, then once boron has segregated to a $Si_{1-x-y}Ge_xC_y$ layer, it should not be able to diffuse out again (assuming the defects are stable). Therefore, an experiment was performed to test the reversibility of the segregation process. The same structure shown in Fig. 3 (to study segregation to $Si_{1-y}C_y$) was first annealed at 850°C for 2 h in $N_2$, as before. In this section, the sample was also subjected to an additional 2 h dry oxidation at 850°C. The purpose of the initial $N_2$ anneal was, as before, to allow the boron to segregate to the $Si_{1-y}C_y$ layer. The second step (oxidation) was designed to drive the carbon out of the $Si_{1-y}C_y$ layer. When the silicon surface is oxidized, it is known that silicon self-interstitials are injected into the sample. These silicon interstitials diffuse down to the $Si_{1-y}C_y$ layer and interact with the substitutional carbon atoms through the following reaction[20]

$$C_S + I \rightarrow C_I \quad [1]$$

where $C_S$ is a substitutional carbon atom, I is a silicon interstitial atom, and $C_I$ is a carbon-silicon interstitial pair, or "interstitialcy." The resulting carbon interstitialcies are very mobile and diffuse quickly compared to the substitutional carbon. As the $Si_{1-y}C_y$ layer is positioned so close to the surface, they can rapidly diffuse to the surface and into the growing oxide. (SIMS profiles confirm that

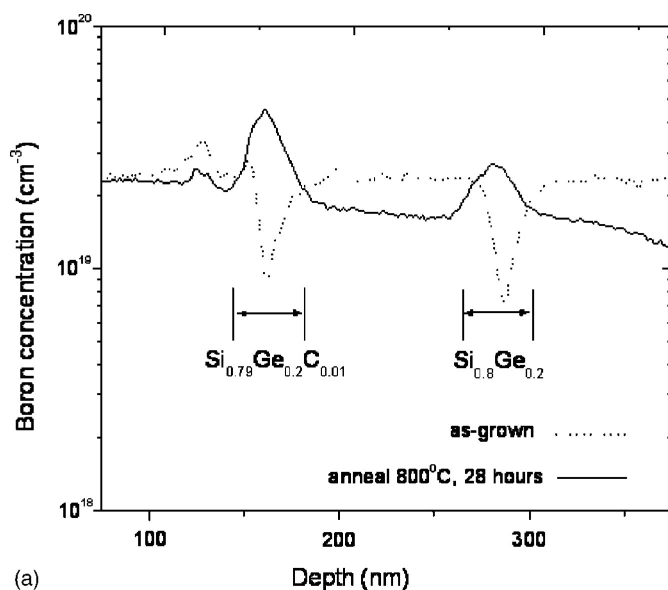


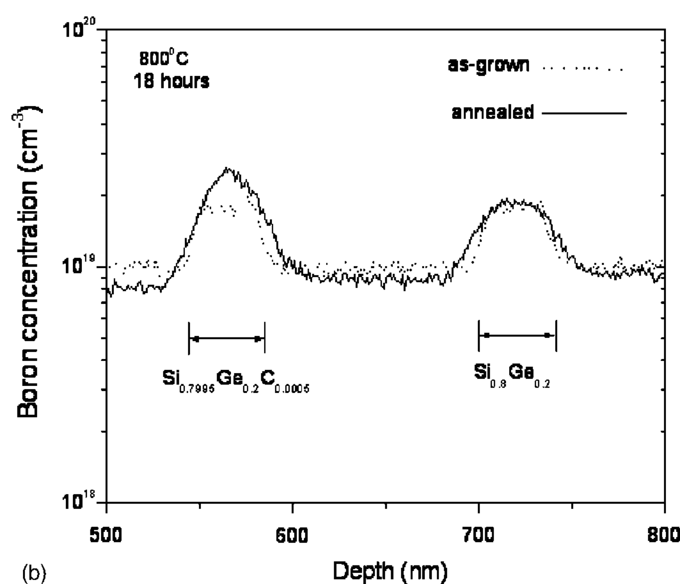


**Figure 2.** SIMS profiles of boron concentration before and after annealing for (a) the high-carbon sample and (b) the low-carbon sample.

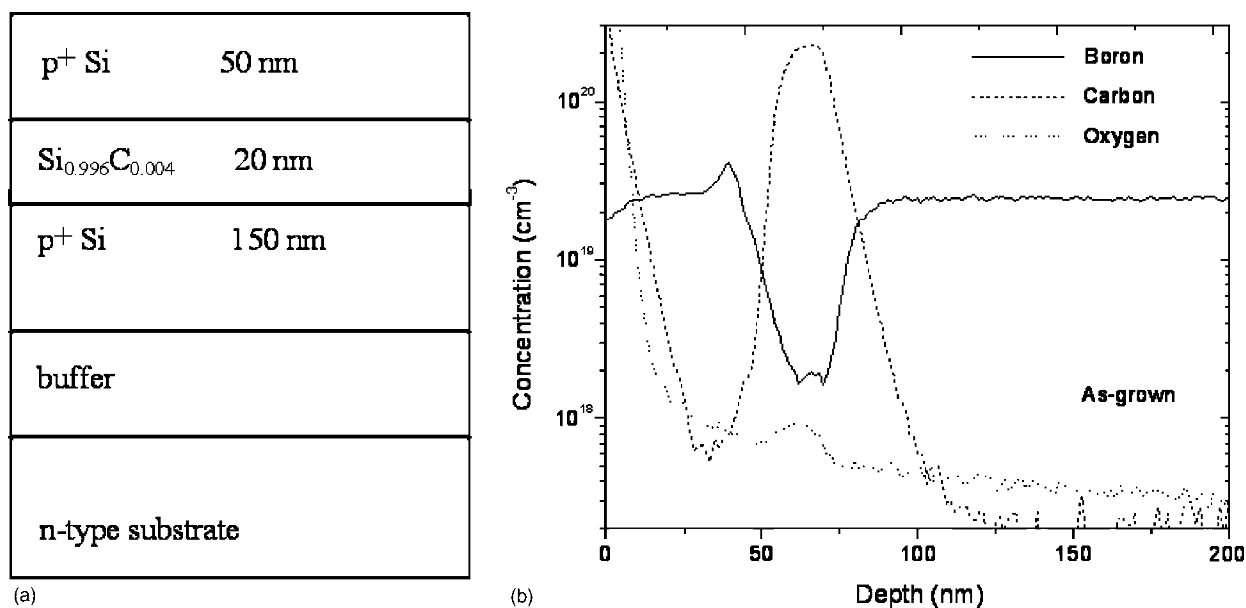


**Figure 3.** (a) Structure and (b) SIMS profiles of as-deposited $Si/Si_{1-y}C_y/Si$ sandwich structure.

carbon is accumulating in the oxide.) It has been previously shown that, by this mechanism, almost all of the carbon can be removed from a $Si_{1-x-y}Ge_xC_y$ layer with the same carbon level (0.4%), thickness, and oxidation conditions.[10] In addition, for the same rate of interstitial injection, the loss of carbon has been shown to be the same for $Si_{1-x-y}Ge_xC_y$ and $Si_{1-y}C_y$ layers.[9]

In Fig. 5, carbon and boron profiles in this sample, which was subjected to both the $N_2$ anneal and oxidation, are compared to the sample from the previous section, which was subjected to only the $N_2$ anneal. It is seen in Fig. 5a that, as anticipated, most of the carbon is removed from the $Si_{1-y}C_y$ layer during the oxidation step. 84% of the integrated carbon has been removed from the region of the original $Si_{1-y}C_y$ layer, with 74% removed from the sample entirely. Figure 5b shows that, at the same time, most of the boron segregation has gone away, with the profile largely flattening out. The decrease near the surface is caused by boron evaporation and/or segregation into the oxide layer on the surface. The ability to reverse the segregation in this structure via the oxidation step argues against the formation of immobile boron-carbon defects as the driving force for the segregation. In particular, it is unlikely that the segregation was caused by SiC precipitates, which were then caused to be removed by the oxidation. The presence of excess interstitials is known to drive the *formation* of SiC precipitates in silicon, not their removal.[21] (Note: A small residual boron peak does remain in the region of the original $Si_{1-y}C_y$ layer; whether this simply has not had enough time to diffuse away, or is potentially associated with defects, is not clear.)

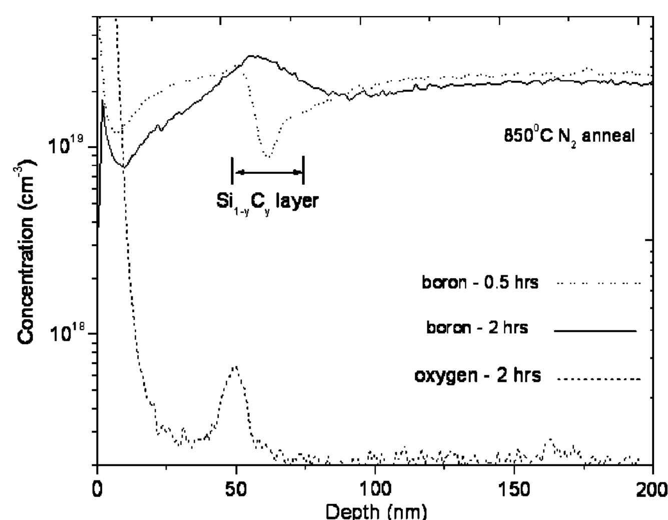


**Figure 4.** SIMS profiles of boron concentration after nitrogen annealing for 0.5 and 2 h at 850°C for the $Si/Si_{1-y}C_y$ sandwich structure. Oxygen concentrations, which have decreased in both the $Si_{1-y}C_y$ and surrounding silicon after 2 h, are also shown.

## Segregation Driven by Gradients of Silicon Interstitial Atoms

We propose that the reaction of carbon with silicon interstitials, and the resulting gradients of interstitials that are produced inside $Si_{1-x-y}Ge_xC_y$ layers, is driving boron segregation into these layers. Carbon (at low concentrations) is a substitutional impurity in silicon and requires the presence of silicon self-interstitials to diffuse.[20] A substitutional carbon atom ($C_S$) pairs with a silicon self-interstitial (I) to form a carbon-interstitial pair, or "interstitialcy" ($C_I$) (Reaction 1), which is mobile and can rapidly diffuse. Eventually it dissociates, with the carbon atom returning to a substitutional site and the silicon interstitial diffusing away. As a result of silicon interstitials being consumed through Reaction 1, and the subsequent diffusion of the carbon-interstitial pairs out of the layers, the population of silicon interstitials is depressed in $Si_{1-x-y}Ge_xC_y$ regions. In the adjacent silicon layers, the dissociation of $C_I$ to form substitutional carbon and silicon interstitials raises the silicon interstitial population there. In the next subsection, we use simulations to model this reaction and diffusion of carbon and interstitial silicon during thermal anneals. In the following subsection, we model the effect that the resulting interstitial profiles have on boron diffusion. Finally, the simulations are compared to data.

*Interstitial undersaturations created by carbon diffusion.*— Previously, a complete model of coupled carbon and point-defect diffusion was developed.[22] Substitutional carbon is assumed to undergo two reactions: Reaction 1, known as the "kick-out" reaction, and the Frank-Turnbull reaction

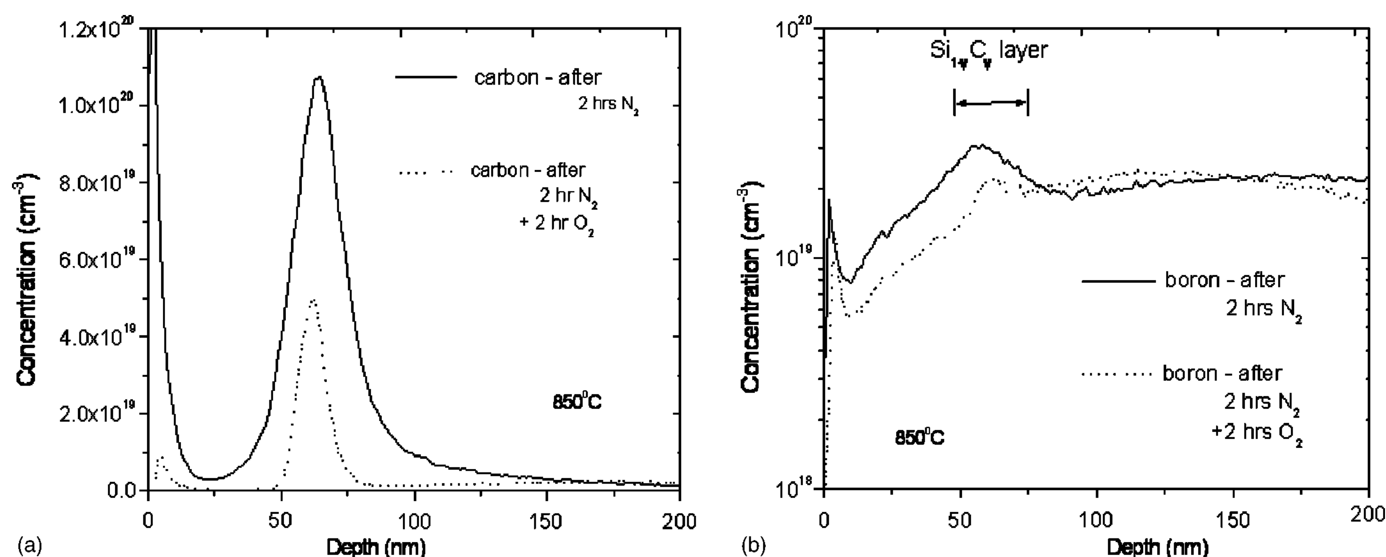


**Figure 5.** SIMS profiles of (a) carbon and (b) boron after 2 h nitrogen anneal at 850°C (solid lines), and after both a 2 h nitrogen anneal and 2 h oxidation at 850°C (dotted lines).[33] The $y$ axis in (a) is on a linear scale.

$$C_S \rightarrow V + C_I \quad [2]$$

where $V$ is the concentration of vacancies in the lattice. This describes substitutional carbon directly forming an interstitialcy and leaving a vacancy behind. The simultaneous reaction and diffusion of all four species ($C_S$,$C_I$, I, and V) was modeled by solving a set of partial differential equations in the PROPHET[23] simulator, using parameters from Ref. 20,24,25. Previously, this model was successfully used to simulate high-concentration carbon diffusion in silicon and $Si_{1-x}Ge_x$ under various conditions. We find that it also can accurately model carbon diffusion (no boron present yet) in our samples. Figure 6 shows the SIMS profile of carbon in a structure identical to the one from the previous section (Fig. 3), except that no boron was present anywhere in the sample. This sample was annealed at 850°C for 2 h in $N_2$, and the resulting data compared with simulations. The profiles match well; in particular, the pronounced diffusion in the tails of the profile, compared to the very slow diffusion in the peak, is modeled very accurately. The good match with the data gives us confidence that the simulation accurately predicts the concentration profile of silicon interstitials in the regions where the carbon is out-diffusing. As seen, the region of high carbon concentration is severely depleted of silicon interstitials, by at least two orders of magnitude compared to the equilibrium value. The adjacent region at a depth of $\sim$300 nm has a slightly enhanced concentration (above the equilibrium value of $1.86 \times 10^{10}\ \text{cm}^{-3}$ at 850°C) due to interstitials being released by the reverse of Reaction 1 in this region.

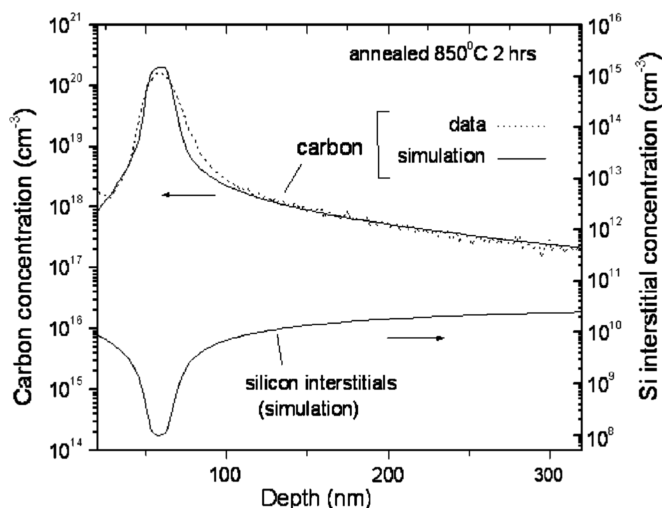


**Figure 6.** Comparison of carbon diffusion SIMS data and simulation for $Si/Si_{1-y}C_y$ structure similar to that in Fig. 3, except with no boron doping, annealed at 850°C for 2 h. The fit is very good, particularly in the tail regions of the carbon profile. Note the large silicon interstitial undersaturation in the $Si_{1-y}C_y$ region predicted by the simulation.

*Theory of boron segregation to regions of low interstitial concentration*.—Boron diffusion depends on silicon interstitials in the same manner as carbon. Similar to Reaction 1, substitutional boron atoms ($B_S$) react with silicon self-interstitials (I) to form mobile boron-interstitial pairs, or "interstitialcies" ($B_I$). It is typically assumed that this reaction and its inverse occur much faster than the diffusion process, and hence can always be considered in equilibrium[26]

$$B_S + I \rightarrow B_I \quad [3]$$

$$kB_SI = B_I \quad [4]$$

where $k$ is a constant. These boron interstitialcies diffuse much faster than substitutional boron, and dominate the process. As a result, the diffusion flux of boron atoms $F_B$ is given by

$$F_B = -D_{BI}\frac{dB_I}{dx} = -D_{BI}\frac{d}{dx}(kIB_s) \quad [5]$$

where Reaction 4 was substituted for the boron interstitialcy concentration, and $D_{BI}$ is their diffusivity. Normalizing the silicon interstitial concentration by its equilibrium value $I_0$, an equilibrium diffusivity $D_{B0}$ can be defined as

$$D_{B0} = -D_{BI}kI_0 \quad [6]$$

Assuming that only a small fraction of boron atoms is paired with interstitials ($B_{Total} = B_S + B_I \approx B_S$), the boron flux can then be expressed as

$$F_B = -D_{B0}\frac{d}{dx}\left(\frac{I}{I_0}B_{Total}\right) \quad [7]$$

If the concentration of silicon interstitials (I) is assumed to be uniform with position, it can be taken out of the derivative, and the diffusivity becomes

$$D_B = D_{B0}\frac{I}{I_0} \quad F_B = -D_B\frac{dB}{dx} \tag{8}$$

where $B = B_{Total}$. In this case, the effective boron diffusivity depends directly on the concentration of silicon interstitials. If it is enhanced, as in oxidation-enhanced diffusion[27] or transient-enhanced diffusion,[28] boron diffusion increases dramatically. If it is decreased, as in a $Si_{1-x-y}Ge_xC_y$ layer, diffusion decreases dramatically.[1] Boron diffusion has actually been used as a measure of the local interstitial concentration in a region.[29]

However, as seen in Fig. 6, the concentration of silicon interstitials is not always constant. At the edges of a $Si_{1-x-y}Ge_xC_y$ layer, there is a steep gradient in the silicon interstitial profile. In this case, Eq. 7 must be expressed as[30,31]

$$F_B = -D_{B0}\frac{I}{I_0}\frac{dB}{dx} - D_{B0}B\frac{d}{dx}\left(\frac{I}{I_0}\right) \tag{9}$$

The first term on the right represents the standard diffusion flux of boron, driven by gradients in boron concentration. The second term states that a flux of *boron* atoms also results from a gradient in *interstitial* atoms, even if no gradient in boron exists. In particular, the flux is in the direction of a negative gradient. As a result, boron is driven from regions of high interstitial concentration to regions of low interstitial concentration, or in our case, into the $Si_{1-x-y}Ge_xC_y$ layer. This provides a mechanism to drive boron segregation into $Si_{1-x-y}Ge_xC_y$ or $Si_{1-y}C_y$ layers from Si based solely on point-defect diffusion considerations.

*Modeling of boron segregation due to interstitial gradients.*— We use the PROPHET simulations described previously to quantitatively model the effect of the interstitial gradients on boron profiles. In particular, we are interested in knowing if the flux produced by the second term in Eq. 9 is powerful enough to drive a significant amount of boron into a $Si_{1-x-y}Ge_xC_y$ layer. All the carbon and interstitial models remained identical to those used for Fig. 6, and boron diffusion was added as described by Eq. 9, using coefficients from Ref. 32 for the equilibrium boron diffusivity $D_{B0}$. In particular, no direct boron-carbon interactions were assumed.

A test structure (not modeled after an experimental sample) was first created in the simulator, consisting of three box-shaped 20 nm $Si_{1-y}C_y$ layers of $y = 0.1$, 0.2, and 0.4% carbon surrounded and separated by 200 nm silicon layers. All silicon and $Si_{1-y}C_y$ layers were initially doped with a uniform boron concentration of $1 \times 10^{19}$ cm$^{-3}$. This was then subjected to a (simulated) 850°C, 14 h anneal. Plots of silicon interstitials and boron after the anneal are shown in Fig. 7, with the location of the $Si_{1-y}C_y$ layers indicated by the arrows. First, note that, as expected, the carbon layers are creating large undersaturations of silicon interstitials. The magnitude of the undersaturation (compared to the adjacent silicon) increases as the carbon concentration increases, starting at ~1.2 times for 0.1% carbon and increasing to ~14 times for 0.4% carbon. Second, and most significantly, strong boron segregation to the regions of interstitial undersaturation is also observed. This increases with carbon level (due to the increasing interstitial undersaturation), starting at 1.6 for 0.1% carbon and increasing to 4.7 for 0.4% carbon. These levels are comparable to the amount of segregation we observed in both our single-crystal and polycrystalline $Si_{1-x-y}Ge_xC_y$ and $Si_{1-y}C_y$ samples, confirming that interstitial gradients alone (without any direct boron-carbon interactions) are powerful enough to drive the boron segregation. However, this is not a true equilibrium segregation effect, as it relies on the nonequilibrium process of carbon reacting with interstitials and out-diffusing. Once the carbon has finished diffusing out of the layer, the interstitial undersaturation, and hence boron segregation, goes away. This is consistent with the findings of the section on reversibility of boron segregation, where after the carbon was removed (in this case by oxidizing the surface) most of the segregation went away.

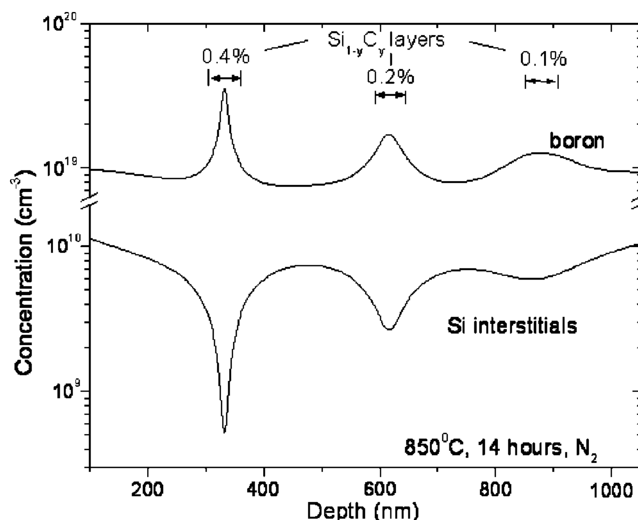


**Figure 7.** Boron and silicon interstitial profiles for the simulation test structure (not experimental data) after 850°C, 14 h anneal, showing strong boron segregation to the regions of low interstitial concentration.

*Comparison of simulation with data.*— These simulations were then applied to model the boron profiles we measured in our experiments. Two samples were chosen for analysis: one with low carbon content (0.05%) and one with high carbon content (0.4%).

The segregation observed in Fig. 2 for a 0.05% $Si_{1-x-y}Ge_xC_y$ layer was first simulated (800°C 18 h). The initial boron and carbon profiles were taken from the SIMS data and used as initial conditions for the simulation. Figure 8 shows a comparison of the modeled and experimental boron profiles after annealing. The agreement is fairly close. However, these results should be interpreted with some caution: germanium effects (which are known to influence both boron diffusion and segregation) are not included in the simulation, nor is the effect of boron on carbon diffusion. For example, we have observed that heavy boron doping (in the $10^{19}$ cm$^{-3}$ range, the same as used for our experiments) can increase the rate of car-

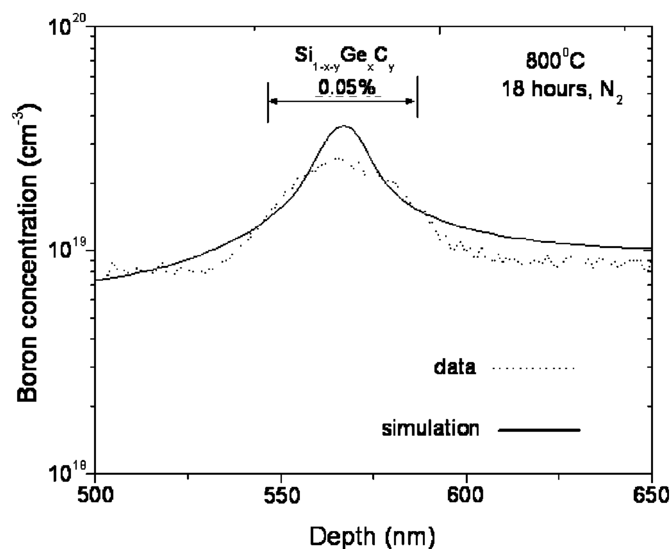


**Figure 8.** Comparison of boron segregation simulation and SIMS data for low-carbon (0.05%) sample annealed at 800°C for 18 h.

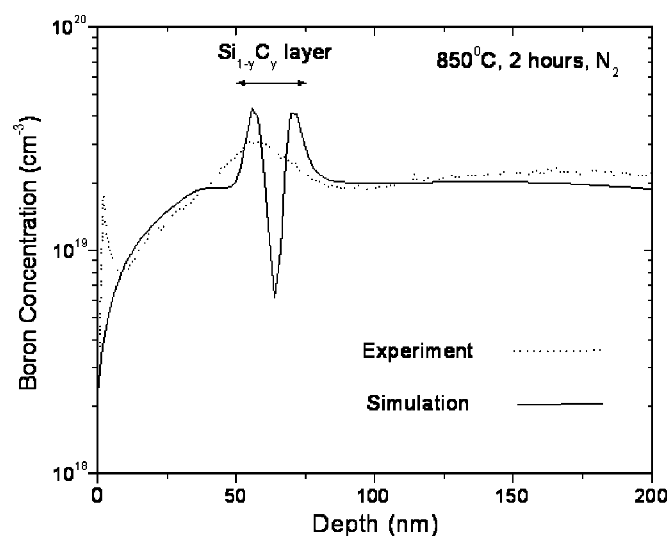


**Figure 9.** Comparison of boron segregation predicted by simulation *vs.* SIMS data for high-carbon (0.4%) sample annealed at 850°C for 2 h.

bon diffusion by a factor of ~2 compared to samples without boron.[33] However, clearly, interstitial gradients created by the carbon are a strong driving force for boron segregation in our samples.

The $Si/Si_{1-y}C_y$ structure used in the section on boron segregation to single-crystal structures, with $y = 0.4\%$, was also simulated in the same manner. Figure 9 shows plots of boron concentration after the 850°C, 2 h anneal, comparing data *vs.* simulation. The simulation again clearly shows that boron is beginning to segregate to the $Si_{1-y}C_y$ layer. However, the model predicts such a low diffusion coefficient in the center of the $Si_{1-y}C_y$ layer that boron cannot finish diffusing into it. But the experimental data show boron segregating all the way into the layer. This discrepancy may be due to inaccuracies in the model parameters, or may be due to the aforementioned effects of boron on carbon diffusion (and hence the interstitial profiles), which are not accounted for in the model. In addition, in the experiment the true boron profiles may not be as uniformly distributed as the data appears, due to broadening in the SIMS measurement. Ultimately, the simulation's prediction that boron does not diffuse all the way into the $Si_{0.996}C_{0.004}$ layer for these anneal conditions may help explain why the segregation seen here is not greater than that in the low-carbon (0.05%) layer (Fig. 8). Although the driving force for segregation is increased with higher carbon (larger interstitial gradient), the diffusivity is also dramatically decreased, thus limiting the ability of boron to move into the layer, and hence the segregation as well.

## Conclusions

In summary, boron segregates from single-crystal silicon to $Si_{1-x-y}Ge_xC_y$ and $Si_{1-y}C_y$ layers during thermal anneals, consistent with studies of polycrystalline material. Segregation coefficients range from 1.7 to 2.9. Boron segregation to a thin $Si_{1-y}C_y$ layer is largely reversible if most of the carbon is removed by an oxidation-enhanced out-diffusion process. This indicates that boron is not segregating to immobile carbon-related traps, such as SiC precipitates. Gradients of silicon interstitial atoms, created during anneals by the substitutional carbon, are a strong driving force for boron segregation. Simulations predict that this effect can drive segregation similar to that seen in experiment; however, a more precise fit to the data may require additional considerations such as the effect of boron on carbon diffusion.

## Acknowledgments

This work was supported by DARPA/ONR N660001-97-8904 and ARO DAA655-98-1-0270.

*Princeton University assisted in meeting the publication costs of this article.*

## References

1. R. Scholz, U. Gosele, J-Y. Huh, and T. Y. Tan, *Appl. Phys. Lett.*, **72**, 200 (1998).
2. L. D. Lanzerotti, J. C. Sturm, E. Stach, R. Hull, T. Buyuklimanli, and C. Magee, *Appl. Phys. Lett.*, **70**, 3125 (1997).
3. I. Ban, M. C. Ozturk, and E. K. Demirlioglu, *IEEE Trans. Electron Devices*, **44**, 1544 (1997).
4. M. Yang, C. L. Chang, M. S. Carroll, and J. C. Sturm, *IEEE Electron Device Lett.*, **20**, 301 (1999).
5. E. J. Stewart, M. S. Carroll, and J. C. Sturm, *Mater. Res. Soc. Symp. Proc.*, , **669**, J6.9 (2001).
6. S. M. Hu, D. C. Ahlgren, P. A. Ronsheim, and J. O. Chu, *Phys. Rev. Lett.*, **67**, 1450 (1991).
7. T. T. Fang, W. T. C. Fang, P. B. Griffin, and J. D. Plummer, *Appl. Phys. Lett.*, **68**, 791 (1996).
8. E. J. Stewart, M. S. Carroll, and J. C. Sturm, *IEEE Electron Device Lett.*, **22**, 574 (2001).
9. M. S. Carroll and J. C. Sturm, *Appl. Phys. Lett.*, **81**, 1225 (2002).
10. M. S. Carroll, J. C. Sturm, E. Napolitani, D. De Salvador, M. Berti, J. Stangl, G. Bauer, and D. J. Tweet, *Phys. Rev. B*, **64**, 073308 (2001).
11. S. Kobayashi, T. Aoki, N. Mikoshiba, M. Sakuraba, T. Matsuura, and J. Murota, *Thin Solid Films*, **369**, 222 (2000).
12. S. M. Hu, *Phys. Rev. B*, **45**, 4498 (1992).
13. R. F. Lever, J. M. Bonar, and A. F. W. Willoughby, *J. Appl. Phys.*, **83**, 1988 (1998).
14. D. De Salvador, M. Petrovich, M. Berti, F. Romanato, E. Napolitani, A. Drigo, J. Stangl, S. Zerlauth, M. Muhlberger, F. Schaffler, G. Bauer, and P. C. Kelires, *Phys. Rev. B*, **61**, 13005 (2000).
15. A. St. Amour, C. W. Liu, J. C. Sturm, Y. Lacroix, and M. L. W. Thewalt, *Appl. Phys. Lett.*, **67**, 3915 (1995).
16. C. L. Chang, L. P. Rokhinson, and J. C. Sturm, *Appl. Phys. Lett.*, **73**, 3568 (1998).
17. L. V. Kulik, D. A. Hits, M. W. Dashiell, and J. Kolodzey, *Appl. Phys. Lett.*, **72**, 1972 (1998).
18. P. Warren, J. Mi, F. Overney, and M. Dutoit, *J. Cryst. Growth*, **157**, 414 (1995).
19. C.-L. Liu, W. Windl, L. Borucki, S. Lu, and X. Y. Liu, *Appl. Phys. Lett.*, **80**, 52 (2002).
20. G. Davies and R. C. Newmann, Carbon in monocrystalline Silicon, in *Handbook on Semiconductors*, T. S. Moss, Editor, p. 1558, Elsevier, Amsterdam (1994).
21. W. J. Taylor, T. Y. Tan, and U. Gosele, *Appl. Phys. Lett.*, **62**, 3336 (1993).
22. M. S. Carroll, Ph.D. Thesis, Princeton University, Princeton, NJ (2001).
23. M. R. Pinto, D. M. Boulin, C. S. Rafferty, R. K. Smith, W. M. Coughran, I. C. Kizilyalli, and M. J. Thoma, *Tech. Dig. - Int. Electron Devices Meet.*, **1992**, 923.
24. H. Bracht, N. A. Stolwijk, and H. Mehrer, *Phys. Rev. B*, **52**, 16542 (1995).
25. H. Bracht, E. E. Haller, and R. Clark-Phelps, *Phys. Rev. Lett.*, **81**, 393 (1998).
26. H. Rucker, B. Heinemann, W. Ropke, R. Kurps, D. Kruger, G. Lippert, and H. J. Osten, *Appl. Phys. Lett.*, **73**, 1682 (1998).
27. H.-J. Gossmann, T. E. Haynes, P. A. Stolk, D. C. Jacobson, G. H. Gilmer, J. M. Poate, H. S. Luftman, T. K. Mogi, and M. O. Thompson, *Appl. Phys. Lett.*, **71**, 3862 (1997).
28. P. A. Stolk, H.-J. Gossmann, D. J. Eaglesham, D. C. Jacobson, C. S. Rafferty, G. H. Gilmer, M. Jaraiz, J. M. Poate, H. S. Luftman, and T. E. Haynes, *J. Appl. Phys.*, **81**, 6031 (1997).
29. M. S. Carroll, J. C. Sturm, and T. Buyuklimanli, *Phys. Rev. B*, **64**, 085316 (2001).
30. C. S. Rafferty, H.-H. Vuong, S. A. Eshraghi, M. D. Giles, M. R. Pinto, and S. J. Hillenius, *Tech. Dig. - Int. Electron Devices Meet.*, **1993**, 311.
31. S. M. Hu, *Mater. Sci. Eng., R.*, **13**, 105 (1993).
32. R. B. Fair, *Impurity Doping Processes in Silicon*, F. F. Y. Wang, Editor, North Holland, Amsterdam (1981).
33. E. J. Stewart and J. C. Sturm, *Mater. Res. Soc. Symp. Proc.*, **765**, 223 (2003).